Reduced kinetic mechanism for methanol combustion in Spark-Ignition engines

Christoffer Pichler[*]*, Elna J. K. Nilsson*

Combustion Physics, Department of Physics, Lund University, P. O. Box 118 SE-221 00, Lund, Sweden

*Corresponding Author

E-mail: christoffer.pichler@forbrf.lth.se

Author Contributions

The manuscript was written through contributions of all authors. All authors have given approval to the final version of the manuscript.

Funding Sources

The authors would like to acknowledge the financial support from the Swedish Research Council via a Young Researcher Grant (Dnr. 2015-05270) and the Swedish Energy Agency.

Keywords: methanol, reduced kinetic mechanism, high pressure, SI-engine, mechanism reduction

ABSTRACT

A reduced kinetic mechanism for methanol combustion at spark-ignition (SI) engine conditions is presented. The mechanism consists of 18 species and 55 irreversible reactions, small enough to be suitable for Large Eddy Simulations (LES). The mechanism was reduced and optimized using the comprehensive mechanism (AramcoMech 2.0) as a starting point, to maintain performance at stoichiometric conditions for the pressure (10-50 bar) and temperature ranges relevant for SI-engine conditions. The mechanism was validated against experimental data for ignition delay at 1050 – 1650 K, flow reactor at 783 K and jet-stirred reactors at 800-1150 K, and simulated validation targets for laminar burning velocity under conditions where no experimental data are available. The mechanism performs well for pollutant formation (CO and CH2O), ignition delay and laminar burning velocity, which are all important properties for LES of engines. Two other reduced mechanisms for methanol combustion, containing around the same number of species and reactions, were tested for comparison. The superior performance of the mechanism developed in the present work is likely a result of that it is specifically produced for the relevant conditions, while the other mechanisms were developed for a limited set of conditions compared to the present work. This highlights the importance of careful selection of reduced mechanisms for implementation in computational fluid dynamics simulations.

1. Introduction

Environmental concerns related to the anthropogenic greenhouse effect and air quality have shifted attention from fossil fuels to renewable alternatives. Methanol (CH_3OH) is a promising fuel that can be produced from various crops, but is also easily produced from non-food sources by gasification of wood, agricultural and municipal wastes[1]. Advantages of methanol, compared to gasoline in spark-ignition (SI) engines, are increased maximum engine power, higher brake thermal efficiency and lower nitrous oxides (NO_x) emissions[2]. On the other hand, methanol also has a few drawbacks: it is explosive in enclosed tanks and soluble in water implying that it is hazardous if spilt in nature[3].

Research on methanol as a fuel include fundamental studies on combustion properties in laboratory systems, as reviewed by Sarathy et al.[4], and engine studies, reviewed by Vancoillie et al.[2]. Engine studies reveal that adding methanol to gasoline in SI-engines decrease carbon monoxide (CO) and unburned hydrocarbons (UHC) emission while increasing emission of formaldehyde (CH_2O) and methanol compared to pure gasoline[5]. Additionally, mixing methanol with diesel in compression ignition (CI) engines increases heat release[6]. Adding methanol to diesel increase NO_x emissions, but decrease smoke opacity, CO and UHC emissions dramatically depending on operating conditions[7]. All engine types that use alcohol or alcohol blends share a common problem of corrosion in the fuel lines and filters, which require use of corrosion resistant material[8].

Pollutant formation is an important concern when developing engines for biofuels. NO_x, UHC, particulate matter (PM), soot and CO are all important emissions from biofuels, similar to traditional fuels[8], but there are also elevated levels of oxygenated intermediates like CH_2O in biofuel exhaust[3, 9, 10]. CH_2O is carcinogenic and produce ground-level ozone[3, 11-13]. CO is a

highly toxic gas that can cause a wide range of symptoms, depending on exposure level, including headache, dizziness, nausea, decreased cognitive function and death[14, 15]. NO_x can enhance production of ground level ozone, it causes breathing problems in humans and acid rain[16]. PM and soot are connected to respiratory problems, heart disease and stroke[17]. UHC can react with NOx to form ground-level ozone, but can also by itself cause drowsiness, eye irritation and coughing[3, 12]. The combined effect of engine pollutants has been shown to correlate to elevated mortality in cities[18].

To make methanol a viable replacement for traditional fuels, further research has to be conducted in order to reduce pollutants and mitigate engine development. The strive towards these goals are accelerated by using Computational Fluid Dynamics (CFD) simulations where accurate chemistry is implemented to obtain flame dynamics and pollutant formation. Large Eddy Simulations (LES) are suitable for modelling of real combustors with explicit chemistry, but comprehensive combustion chemistry mechanisms are to extensive to be computationally feasible[19]. A typical limitation is in the range 20-30 species, and some 40-80 reactions, which is regarded as sufficient to describe combustion of hydrocarbon fuels[20]. Oxygenates like alcohols, however, have a larger number of possible reaction paths which may present a challenge in mechanism reduction. Computational cost can be substantially decreased by use of global reactions like the 5-step mechanism by Yalamanchili et al.[21], but this significantly limit the applicability since pollutant formation cannot be predicted.

Comprehensive kinetic mechanisms for methanol combustion, developed prior to 2013[22-24], have been reviewed by Sarathy et al.[4]. More recently, highly detailed mechanisms with extensive updates and validation for methanol have been published, i.e. the mechanism of Konnov and co-workers[25] and the AramcoMech 2.0[26]. The mechanism by Li et al.[24] was implemented in a

coupled chemistry and LES study of methanol ignition in an SI-engine, by Zhen et al.[27]. However, as mentioned previously, a comprehensive mechanism is in general too computationally expensive to be used for more complex LES systems.

Reduced mechanism for methanol combustion, with number of species and reactions suitable for LES are few, and their applicability are limited. Fernández-Tarrazo et al.[28] presented a mechanism with 21 species involved in 14 reversible and 26 irreversible reactions. The mechanism is developed for fuel oxidation, auto-ignition and premixed flame propagation in spray-combustion conditions, typically found in a CI-engine, up to 10 bar, equivalence ratio of 0.5 – 2.0 and auto-ignition temperatures in the range 1000-3000 K. The mechanism of Seiser et al.[29] contains 18 species and 26 irreversible reactions, models ignition delay and strain rate up to 20 bars, for auto-ignition temperature 1500-1900 K and oxidizing temperature between 1100-1400 K. Lindstedt and Meyer[30] improved a pre-existing model, with 23 species and 19 reversible reactions, and validated it for laminar burning velocity at 318 K and atmospheric pressure, ignition delay and species profiles at atmospheric and low pressure conditions. The reduced mechanism by Liao et al.[31], consisting of 19 species and 40 reversible reactions, is validated against experimental data for laminar burning velocity at 318 – 480 K, for ignition delay at equivalence ratio of 0.375 – 6.0, temperature of 1545 – 2180 K and pressure in the range of 0.18 – 0.46 MPa and profiles of pollutants and major species at 800 – 1200 K.

None of the mentioned reduced mechanisms for methanol combustion are developed for the full range of conditions relevant for SI-engines. In the present work, a reduced mechanism is presented, containing 18 species and 55 irreversible reactions, developed for SI-engine conditions. The focus is on high accuracy for important pollutants (CO, CH_2O), ignition delay and laminar burning velocity at common SI-engine conditions.

2. Mechanism development

The accuracy of a size-reduced mechanism is inevitably inherited from the more detailed mechanism it is constructed from, and thus it is crucial to select a highly detailed and comprehensive reference mechanism[20]. This is particularly important when the reduced mechanism need to accurately represent production and consumption of intermediate chemical species to predict pollutant formation, since the dominating reaction routes need to be retained. For a reduced mechanism to be computationally efficient it needs to be sufficiently small, but another important aspect is that its mathematical stiffness should be as low as possible. Mathematical stiffness is commonly related to the presence of a wide span of chemical timescales[20]. Fast depleting radicals reaching quasi steady state and fast reversible reactions in partial equilibrium are the main problems, in particular for reactions of long chained fuels.

The reduction approach used in the present work do not explicitly address the stiffness issue. However, the mechanism size as well as the total simulation time are taken into consideration and thus a good balance between performance, low number of reactions and low stiffness can be found without considering any one of these trait individually.

The reduced mechanism is developed to accurately reproduce the results of a detailed mechanism at the conditions relevant for SI-engines. This results in a smaller mechanism than one that is designed to mimic the detailed mechanism at all conditions, but it is important to keep in mind that it might not produce accurate results outside the specified range. The pressure in an SI-engine at top dead centre can be up to 200 bar, and the temperature of the unburnt gas can be up to 600 K. An SI-engine combusts premixed gas, commonly with composition close to stoichiometric conditions, but it could also be operated at lean fuel-air mixtures.

The proposed reduced mechanism was derived from the detailed mechanism by Li et al.[26], AramcoMech 2.0, consisting of 493 species and 2716 reversible reactions. This mechanism can model a wide array of fuels in the C1 to C4 range and has been validated for methanol combustion under conditions relevant for SI-engines, where reliable experimental data exists[32]. Because of the comprehensiveness of AramcoMech 2.0, it is suitable as a starting point for mechanism reduction.

The reduction method, Ant Colony Reduction (ACR), used in this work is a semi-stochastic approach developed from a metaheuristic algorithm called Ant Colony Optimisation[33, 34]. The reduction is made against a carefully selected range of targets, representing conditions at which the final mechanism need to predict ignition, flame propagation and concentrations of important species. The target conditions used for mechanism development are given in the first section of Table 1. Some of the development targets (FR1, JSR1, JSR2) correspond to experimental datasets for which reference is given in the table. A more extensive table including mixture compositions are available as Table S1 in Supplementary material.

Using the ACR reduction a subset of 45 reversible reactions was obtained, preserving all enhancement factors and pressure dependence formulations for each reaction identically to how it is implemented in AramcoMech 2.0. The reactions in this first version of the reduced mechanism was split into 90 irreversible reactions using the program MechMod[35]. The AramcoMech 2.0 treat pressure dependence using the PLOG approach[36], and the reduced mechanism contained one reaction of this type, $CH_3 + OH \leftrightarrow CH_2OH + H$. MechMod cannot convert reactions with plog-expressions and before it could be used, the pressure dependence in the reaction was modified to a TROE falloff form instead of plog-expressions. The 90 reactions mechanism was processed by another Ant Colony Reduction step that removed unnecessary

reactions to yield a final reaction set consisting of 55 irreversible reactions. In this step four reactions were completely removed, 27 reactions were retained in the dominating direction only and 14 remained with both directions intact. Arrhenius' A-factors for reaction rates with large experimental uncertainties were in the final reduced mechanism optimised using an adapted form of Genetic Algorithms[37]. All reactions that were modified in the optimization are listed in Table S3, available as Supplementary information, and both original (i.e. AramcoMech 2.0) and optimized reaction rate constants are given. Since the reduced mechanism was constructed using ACR and contains 55 irreversible reactions, it is referred to in this article as ACR55.

Table 1presents conditions used for development, first section, and validation, second section, of the reduced mechanism. A more extensive table including mixture compositions are available as Table S1 in Supplementary material. An SI engine operates at near stoichiometry and the reduced mechanism is developed for these conditions[38]. Conditions were selected based on that the pressure inside an engine cylinder at medium load for compression ratio of 8:1 to 9.5:1 is in the range 10 – 50 bar when combustion occurs, and the temperature at ignition is around 300 – 600 K[38].

Table 1. Relevant combustion conditions for simulations in an SI-engine. Each case is near stoichiometry, uses CH_3OH as fuel and O_2 as the oxidizer. Simulation types are specified as Ignition Delay Time (IDT), Freely Propagating flame (FP), Jet-Stirred Reactor (JSR) or Flow Reactor (FR). References to experimental work at similar conditions are specified when available.

Name	P (bar)	T (K)	Dilute	Ref
Development dataset				
FR1	15.0	783	N_2	[22]

JSR1	10.0	800-1130	N_2	[32]
JSR2	20.0	800-1150	N_2	[32]
IDT1	10.0	1150-1600	N_2	
IDT2	35.0	1100-1550	N_2	
IDT3	50.0	1050-1500	N_2	
FP1	50.0	500	N_2	
FP2	40.0	500	N_2	
FP3	30.0	500	N_2	
FP4	20.0	500	N_2	
FP5	10.0	500	N_2	
FP6	30.0	400	N_2	
FP7	30.0	300	N_2	
Validation dataset				
IDT4	20.0	1016-1208	N_2	[32]
IDT5	30.9	963-1125	N_2	[32]
IDT6	49.3	989-1214	N_2	[32]
IDT7	10.2	999-1273	Ar	[32]
IDT8	49.2	994-1295	Ar	[32]
IDT9	10.1	1091-1426	Ar	[32]
IDT10	13.0	899-1211	N_2	[39]
IDT11	40.0	820-1108	N_2	[39]
IDT12	10.1	1073-1299	Ar	[40]
IDT13	10.5	1071-1610	Ar	[40]
FP8	10.0	373	N_2	[41]

The development dataset, first part of Table 1, was selected to cover the relevant temperature and pressure ranges and used to construct and optimise the reduced kinetic model using

AramcoMech 2.0 as a starting point. The development targets for mechanism reduction need to include a relevant range of chemical regimes, captured in various types of experiments and simulations. The laminar burning velocity targets (10-50 bar, 300-500 K) were selected since this property govern the high temperature chemistry of combustion, jet-stirred reactor (10-20 bar, 800-1150 K) and flow reactors (15 bar, 783 K) are valuable since they represent oxidation chemistry important for pollutant formation, and ignition delay (10-50 bar, 1050-1600 K) capture reactivity over a wide range of temperatures[20]. For parts of the validation dataset experimental data exists, as referenced in Table 1. The validation set used to validate the final mechanism consists of the development set and additional datasets for which experimental results exist at SI-engine conditions, these datasets are briefly outlined in the following paragraph.

The experimental data by Burke et al.[32], Fieweger et al.[39] and Noorani et al.[40] were used to validate ignition delays at stoichiometric conditions with pressures between 10–50 bars. Held and Dryer[22] made an experimental study of species profiles for major species in a flow reactor at stoichiometric conditions and pressure of 15 bars that was used to develop and validate the mechanism for pollutant formation. The jet-stirred reactor experiments by Burke et al.[32] were used to validate the model in the temperature range of 800–1150 K and at 10 and 20 bars pressure for formation of major species CH_3OH, CO_2 and O_2, and selected pollutants CO, CH_2O and H_2. Most laminar burning velocity experiments are conducted near atmospheric pressure for methanol and was therefore not included in the present development or validation set. In addition, the scatter in experimental data is significant, with as much as 15 cm/s at maximum laminar burning velocity. As discussed by Vancoillie et al.[42] this is to some extent a result of flame instabilities and insufficient or no corrections for stretch effects, and many of the older studies can be considered unreliable. The only recent published laminar burning velocity within

the range of conditions relevant for the present work is a study by Beeckmann et al.[41, 43] investigated equivalence ratio dependency of laminar burning velocity at 10 bar and 373 K, using a methanol-air mixture. Due to the lack of experimental data for laminar burning velocity in the relevant range of conditions, the main validation for this property is only towards the detailed mechanism AramcoMech 2.0, representing the best estimate of the laminar burning velocity.

All simulations were conducted using Chemkin[36] with initial conditions described in Table 1. The one-dimensional freely propagating flame simulations were carried out using mixture-averaged diffusion, with around 500 grid points per simulation for AramcoMech 2.0 and around 350 grid points for the reduced models. The automated grid generation of Chemkin ensures a grid independent solution by checking that the gradient and curvature change between two adjacent points are below 2.5 %. Ignition simulations were conducted using 0D homogenous reactor with constant volume. Similar to ignition simulations, the flow reactor used the 0D homogenous reactor, but with constant pressure instead of volume. The jet-stirred reactor was modelled using the Steady State Solver with fixed gas temperature and residence time 0.5 s (JSR1) and 1.0 s (JSR2). The ACR55 mechanism in Chemkin format is available as Supplementary Material.

3. Results

As outlined above the ACR55 mechanism was developed to agree with a selected set of ignition delay times, laminar burning velocities and species profiles, and as a result of this the mechanism will always produce results in close agreement with the reference mechanism AramcoMech 2.0 for these conditions. In the present section we evaluate the performance of ACR55 in comparison with other reduced mechanisms, to selected sets of experimental data. For

some important conditions where no experimental data exist the mechanisms are discussed in relation to each other. Selected results are presented here and additional figures are available as Supplementary Material. In all the figures, results from ACR55, AramcoMech 2.0 and the mechanisms of Liao et al.[31] and Fernández-Tarrazo et al.[28], are presented. The latter two are from here on called Liao and Fernandez, and they were selected for comparison since their size is similar to ACR55, and available as full mechanisms in the literature. As can be seen in Figures 1-9, ACR55 demonstrates superior performance at SI-conditions, in comparison to Liao and Fernandez. The results are expected, since ACR55 is specifically tailor-made for these conditions.

All simulations in the reduction step were conducted in air or air-like conditions (using nitrogen (N_2) as a diluent gas), but a few experiments in the validation set were conducted using argon (Ar) as a diluent gas, and in these cases Ar was added to the species list of the proposed mechanism alongside the enhancement factor identically to how they are implemented in AramcoMech 2.0.

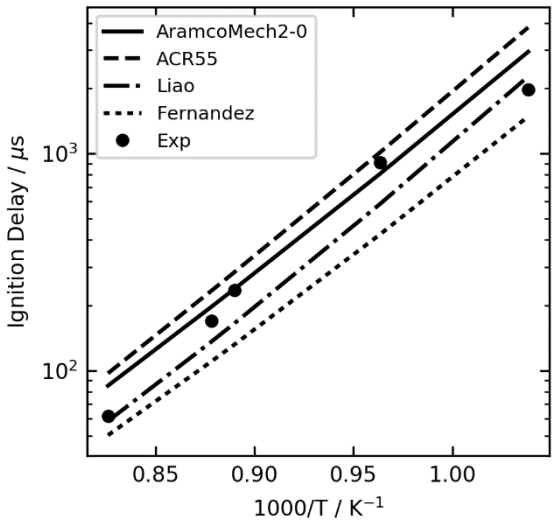

Figure 1. Ignition delay for stoichiometric conditions of CH_3OH and O_2 with N_2 as diluent gas at 13.00 bar (condition IDT10). The circles are experimental data by Fieweger et al. [39]. Experimental data points are digitised from figures in the original publications.

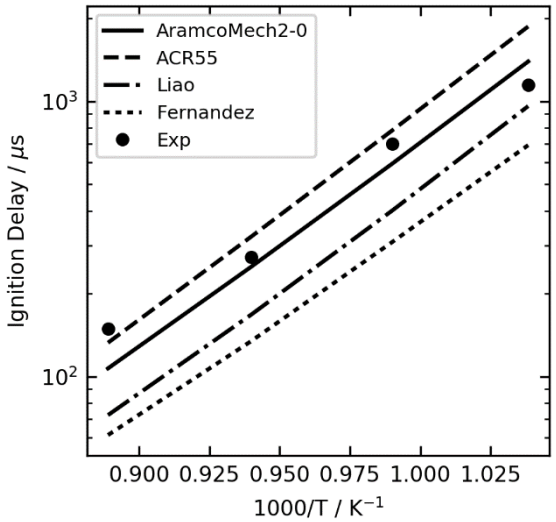

Figure 2. Ignition delay for stoichiometric conditions of CH_3OH and O_2 with N_2 as diluent gas at 30.88 bar (condition IDT5). The circles are experimental data by Burke et al. [32]. Experimental data points are digitised from figures in the original publications.

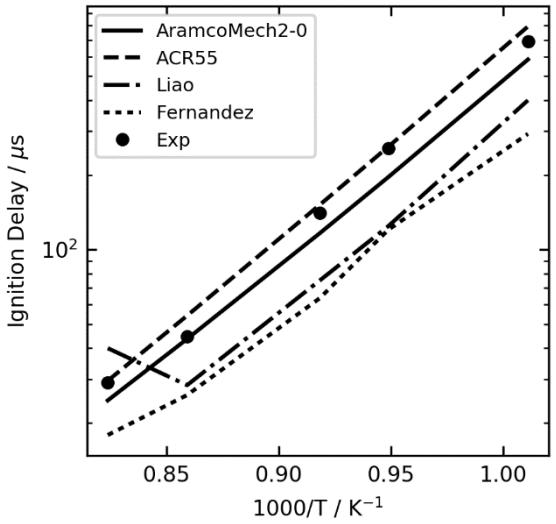

Figure 3. Ignition delay for stoichiometric conditions of CH3OH and O2 with N2 as diluent gas at 49.27 bar (condition IDT6). The circles are experimental data by Burke et al.[32]. Experimental data points are digitised from figures in the original publications.

Ignition delays (in this article defined as global maximum of OH concentration) at various pressures (13-49 bar) are presented in Figures 1-3, with additional results presented in Figures S1-S7, available in the Supplemental material. In the experimental works the ignition delay time was determined using the pressure rise or luminosity, but in the simulations OH is used as a unified comparison of the mechanisms. Davidson and Hanson[44] present an evaluation of various definitions of ignition delay and concludes that at the conditions of relevance in the present work, the common definitions deviate by at most 2%. All three reduced mechanisms, ACR55, Fernandez and Liao, are essentially in agreement with the experimental results of the 13 bar case by Fieweger et al.[39] (Figure 1), considering reasonable experimental scatter and uncertainties based on information given by Fieweger et al.[39] and general considerations about shock-tube experiments discussed by Davidson and Hanson[44]. However, it is only AramcoMech 2.0 and

ACR55 that are in satisfactory agreement with the two high pressure data sets from Burke et al.[32] (Figures 2, 3). The highest temperature data point at condition IDT6 for Fernandez and Liao is shifted upwards, since the OH profile does not have a well-defined peak, but instead the equilibrium value is close to the maximum value at this temperature.

The chemical reactions governing ignition delay times have been identified using sensitivity analysis for ignition delay at 1100 K at 13 and 49 bar. Sensitivity plots for the three reduced mechanisms are available as Figs S15-S17 in the supplementary material. The mechanisms share the three dominating reactions: $CH_3OH+HO_2=CH_2OH+H_2O_2$, $H_2O_2+M=2OH+M$ and $2HO_2=H_2O_2+O_2$, where the first two promote ignition and the third inhibit ignition. The reaction rate constants of the three reactions are, however, different in the three mechanisms (see Table S2 in Supplementary material) and from this the difference in reactivity between the mechanisms, evident from Figs. 1-3, can be deduced. The most reactive mechanism, i.e. with shortest ignition delay time, is Fernandez, which has a pre-exponential factor twice as high as the other mechanisms for the main ignition promoting reaction. The relatively high reactivity of Liao is a result of a comparably low reaction rate for the damping self-reaction of HO_2.

Experimental laminar burning velocities of methanol/air flames have been difficult to reproduce using modelling, as discussed by, among others, Beeckmann et al.[41, 43] and Nauclér et al.[45]. Most studies have been at atmospheric pressures and the only experimental data point for laminar burning velocity in the range of relevance for the present work is at 373 K and 10 bar, by Beeckmann et al.[41]. They present an experimentally determined value of around 34 cm/s at stoichiometric conditions, while AramcoMech 2.0 predicted 19.4 cm/s, ACR55 predicted 19.9 cm/s (closely resembling AramcoMech 2.0), Liao 21.3 cm/s and Fernandez predicted 22.1 cm/s.

All the numerical models under predict the laminar burning velocity, similar to the numerical part of the study of Beeckmann et al.[41, 43].

A comparison of simulations is used as a further evaluation of laminar burning velocities, presented in Figures 4 and 5. Figure 4 shows the trend of laminar burning velocity at constant temperature and varying pressure (10-50 bar), with the correlation of Vancoillie et al.[42] plotted together with the simulations. In this figure it can be seen that the mechanism by Liao is on average 10 % above the prediction of laminar burning velocity by AramcoMech 2.0. The mechanism by Fernandez shows a different overall trend than the others with less pronounced decrease with pressure. The correlation shows a trend that is higher than any of the mechanisms, with a higher relative agreement at high pressure and low temperature. A sensitivity analysis was performed for the three reduced mechanisms at pressures 10 and 50 bar, to reveal the most important reactions, as presented in Figures S18-S20 in the supplementary material. The mechanisms share the three most sensitive flame promoting reactions for 10 bar: $O_2+H=O+OH$, $CO+OH=CO_2+H$ and $HO_2+H=2OH$, but with different relative importance. For the 50 bar case the same reactions are important, but to various extent in competition with $CH_3OH+HO_2=CH_2OH+H_2O_2$.

Figure 5 shows the trend of laminar burning velocity at constant pressure and varying temperature (300-500 K), and the results of all the reduced mechanisms share a similar trend.

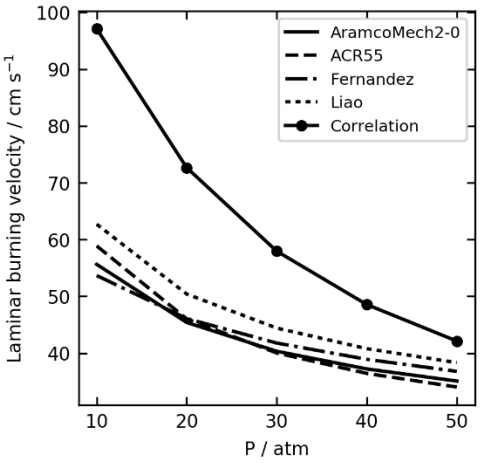

Figure 4. Laminar burning velocity for stoichiometric conditions of CH_3OH and air using unburnt gas temperature of 500 K (FP1-5) at varying pressure.

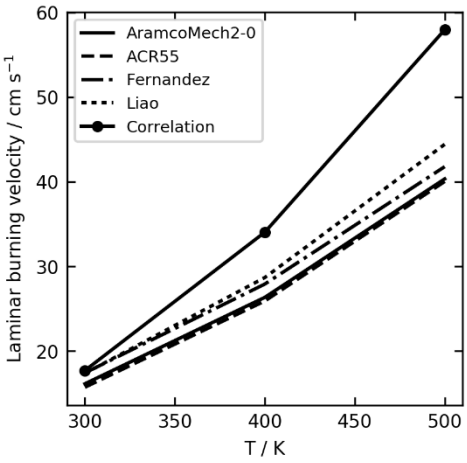

Figure 5. Laminar burning velocity for stoichiometric conditions of CH_3OH and air at 30.00 bar (FP3, FP6 and FP7) using varying unburnt gas temperature.

Pollutant formation at various temperatures in jet-stirred reactor simulations (JSR1 and JSR2) are presented in Figures 6-9, while results for flow reactor simulations (FR1) are available as Figures S8-S14 in the Supplementary material. Reactants CH_3OH and O_2, and the final product

CO_2, are presented in Figures 6 and 7 for 10 and 20 bars, respectively. All mechanisms capture the overall trends for these species quite well, but it is clear that the discrepancies are larger at low temperatures, in particular for the mechanism of Fernandez. The two main pollutants of interest for methanol combustion are CH_2O and CO (Figures 8, 9). All the mechanisms perform well at higher temperatures for CH_2O, but under-predicts the experimental results below 900 K. ACR55 and Liao show a similar trend, both for 10 bar (JSR1) and 20 bar (JSR2) almost predicting the results equally well as AramcoMech 2.0. For CO, all the models except Fernandez show a similar trend, with Fernandez performing better at high temperature and worse at low temperature. At 20 bar pressure (JSR2), none of the mechanisms have the correct quantitative predictions, but the qualitative trends are in line with the experimental trend.

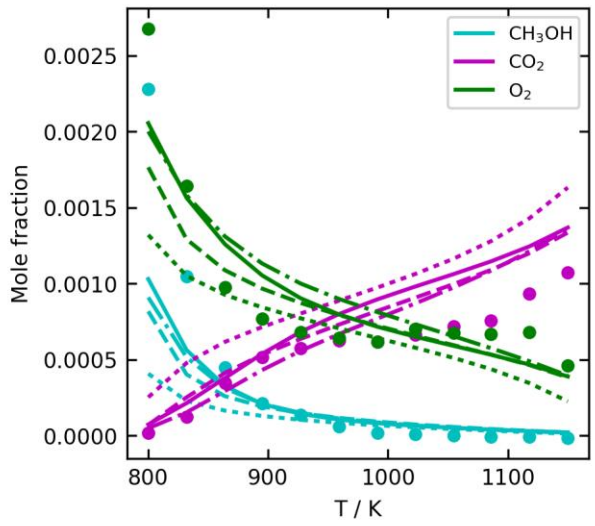

Figure 6. Jet-stirred reactor results of major species for stoichiometric conditions of CH_3OH and O_2 at 10.0 (condition JSR1) at varying temperature with residence time (τ) of 0.5. Circles are experimental data by Burke et al.[32]. Solid line is AramcoMech2.0, dashed line is ACR55, semi-

dotted is Liao and the dotted line is Fernandez. Experimental data points are digitized from figures in the original publications.

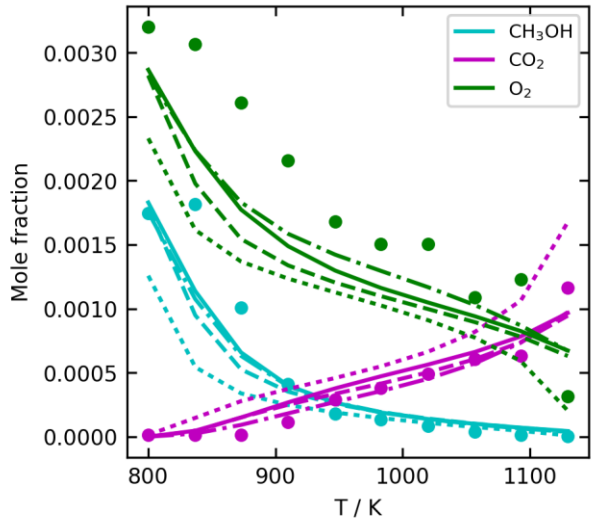

Figure 7. Jet-stirred reactor results of major species for stoichiometric conditions of CH3OH and O2 at 20.0 (condition JSR2) at varying temperature with residence time (τ) of 1.0. Circles are experimental data by Burke et al.[32]. Solid line is AramcoMech2.0, dashed line is ACR55, semi-dotted is Liao and the dotted line is Fernandez. Experimental data points are digitised from figures in the original publications.

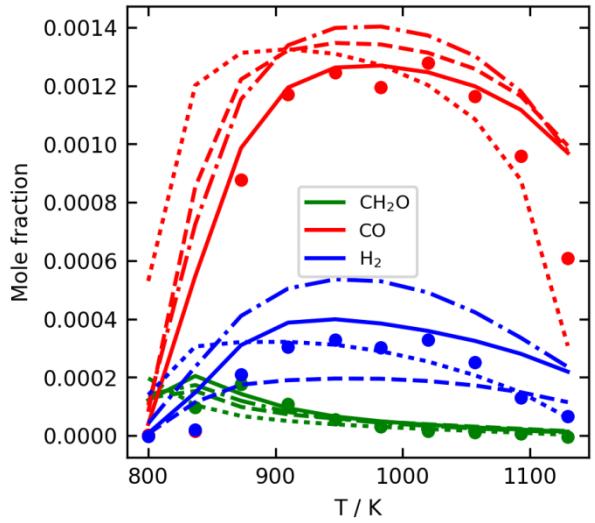

Figure 8. Jet-stirred reactor results of minor species for stoichiometric conditions of CH_3OH and O_2 at 10.0 (condition JSR1) at varying temperature with residence time (τ) of 0.5. Circles are experimental data by Burke et al.[32]. Solid line is AramcoMech2.0, dashed line is ACR55, semi-dotted is Liao and the dotted line is Fernandez. Experimental data points are ~~digitised~~digitized from figures in the original publications.

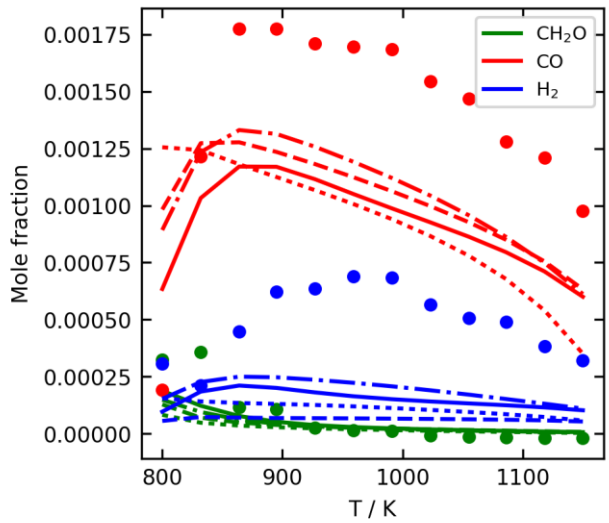

Figure 9. Jet-stirred reactor results of minor species for stoichiometric conditions of CH_3OH and O_2 at 20.0 (condition JSR2) at varying temperature with residence time (τ) of 1.0. Circles are

experimental data by Burke et al.[32]. Solid line is AramcoMech2.0, dashed line is ACR55, semi-dotted is Liao and the dotted line is Fernandez. Experimental data points are ~~digitised~~digitized from figures in the original publications.

4. Chemistry

The purpose of a reduced mechanism, in contrast to a global mechanism containing just a few reaction steps, is that accurate representation of chemistry should be preserved for the important species. To understand the time resolved chemistry using rate of production, a single case from the jet-stirred reactor case was chosen. In Figure 10, the top eight reactions, based on absolute rate of production of CH_2O, is shown for both AramcoMech 2.0 and ACR55 for a flow reactor simulation at 897 K using condition JSR2 in Table 1. The same four reactions are in the top for both mechanisms and has similar rate of production values, indicating that the important chemistry is still present in the reduced mechanism. AramcoMech 2.0 only contains reversible reactions while ACR55 contains irreversible reactions. This difference makes a quantitative comparison ambiguous, but the qualitative conclusion regarding the chemistry can still be drawn. Furthermore, since it is absolute rate of production, both directions of the reversible reaction will have the same rate of production for AramcoMech 2.0, but will have be different for ACR55. This can be seen once in Figure 10 and twice in Figure 11.

During reduction, 219 reversible reactions involving CH_2O was reduced to 17 irreversible reactions. Similarly, 138 reversible reactions involving CO were reduced to 6 irreversible reactions. Figure 11 shows the absolute rate of production for the same case as Figure 10, but for CO instead of CH_2O.

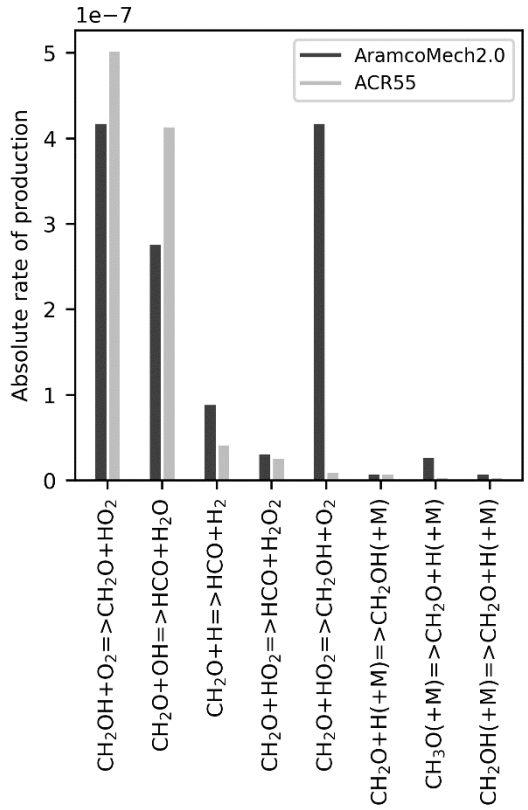

Figure 10. Absolute rate of production for top ten active reactions for CH_2O formation using flow reactor simulation at 897 K and 20 bar pressure, chosen as a specific temperature case of JSR2.

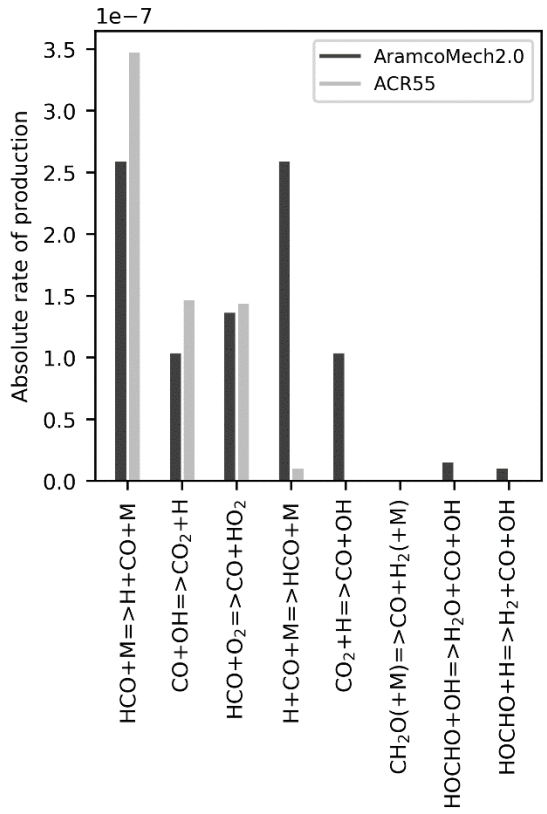

Figure 11. Absolute rate of production for top ten active reactions for CO formation using flow reactor simulation at 897 K and 20 bar pressure, chosen as a specific temperature case of JSR2.

The mechanism of Liao et al., which is slightly larger than ACR55, performs quite well at SI-conditions which was demonstrated in Section 3 and is in better agreement with ACR55 than the Fernandez mechanism. Comparing the mechanism of Liao (40 reversible reaction) with the present work show that the same species are used in both, with the exception of argon (Ar) that is added to Liao, but not to ACR55 in the original version. However, the choice of reactions is slightly different between the mechanisms. ACR55 include more fuel decomposition reactions, especially with CH_3O as a product, than Liao. Another important difference is that Liao contains fewer pressure dependent reactions (only for CH_3OH, CH_4 and HO_2 decomposition), whereas ACR55 have decomposition of CH_3OH, CH_2OH, CH_3O, CH_2O, H_2O_2 and HO_2 alongside

pressure dependent reactions involving CH_2OH. These differences in mechanism structure is most likely due to Liao et al.[31] developing their mechanism for mostly atmospheric and up to a few bar of pressure, but a wide range of equivalence ratios, while ACR55 is developed to predict pollutant formation at high pressure (10-50 bars) and only stoichiometric conditions. The mechanisms thus cover different chemical regimes.

5. Conclusions

Bridging the gap between comprehensive chemical kinetics and CFD simulations is important and the proposed mechanism is an effort to construct the first methanol mechanism designed specifically for a wide range of SI engine conditions. The mechanism was successfully reduced from a comprehensive mechanism using a novel method, and, with 18 species and 55 irreversible reactions, it has a reasonable size for LES of complex systems. It is not recommended to use the mechanism outside of the validation range, since the results can be different from a comprehensive mechanism.

The mechanism reduction and optimization method, using Ant Colony Optimization and Genetic Algorithm, ensure that the reduced mechanism ACR55 is in agreement with the comprehensive mechanism AramcoMech 2.0, over the selected range of conditions. Additional validation towards experimental datasets showed similar agreement as the AramcoMech 2.0. The performance of ACR55 was superior to the other two investigated reduced mechanisms, that were developed for different, and in some aspects more limited, range of conditions. Closer comparison to the mechanism of Liao et al.[31] did, however, show that the two mechanisms have many similarities.

The simulation times for all freely propagating flames (FP1-FP7) in the reduction set were equally long for ACR55 and Liao, around 0.4% of the computational time of AramcoMech 2.0.

Similarly, simulation times for all the non-flame simulations (FR1, JSR1, JSR2, IDT1-IDT3) in the reduction set were almost the same for ACR55 and Liao, around 24.6 % of the computational time of AramcoMech 2.0. Fernandez was not included in the time comparison, since it has convergence issues when using the same set of grid parameters that worked for the other mechanisms.

Although there is good agreement between the mechanism and the existing experimental validation targets presented in Section 3, a weakness is that experimental laminar burning velocities at elevated pressures and temperatures are not available at the moment. Consequently, when the experimental data is available, the mechanism should be updated to incorporate the new information to further increase the accuracy of its predictions.

Acknowledgements

The authors would like to acknowledge the financial support from the Swedish Research Council via a Young Researcher Grant (Dnr. 2015-05270) and the Swedish Energy Agency.

References

1. Bromberg, L.; Cheng, W., Methanol as an alternative transportation fuel in the US: Options for sustainable and/or energy-secure transportation. *Cambridge, MA: Sloan Automotive Laboratory, Massachusetts Institute of Technology* **2010**.
2. Vancoillie, J.; Demuynck, J.; Sileghem, L.; Van De Ginste, M.; Verhelst, S.; Brabant, L.; Van Hoorebeke, L., The potential of methanol as a fuel for flex-fuel and dedicated spark-ignition engines. *Applied Energy* **2013,** 102, 140-149.
3. Agarwal, A. K., Biofuels (alcohols and biodiesel) applications as fuels for internal combustion engines. *Progress in energy and combustion science* **2007,** 33, (3), 233-271.
4. Spence, R.; Wild, W., The vapour pressure curve of formaldehyde, and some related data. *Journal of the Chemical Society* **1935**, 506-509.
5. Liu, S.; Clemente, E. R. C.; Hu, T.; Wei, Y., Study of spark ignition engine fueled with methanol/gasoline fuel blends. *Applied Thermal Engineering* **2007,** 27, (11), 1904-1910.
6. Huang, Z.; Lu, H.; Jiang, D.; Zeng, K.; Liu, B.; Zhang, J.; Wang, X., Combustion behaviors of a compression-ignition engine fuelled with diesel/methanol blends under various fuel delivery advance angles. *Bioresource technology* **2004,** 95, (3), 331-341.
7. Sayin, C.; Ilhan, M.; Canakci, M.; Gumus, M., Effect of injection timing on the exhaust emissions of a diesel engine using diesel–methanol blends. *Renewable energy* **2009,** 34, (5), 1261-1269.
8. Westbrook, C. K., Biofuels combustion. *Annual review of physical chemistry* **2013,** 64, 201-219.
9. Stump, F. D.; Knapp, K. T.; Ray, W. D., Influence of ethanol-blended fuels on the emissions from three pre-1985 light-duty passenger vehicles. *Journal of the Air & Waste Management Association* **1996,** 46, (12), 1149-1161.
10. Jacobson, M. Z., Effects of ethanol (E85) versus gasoline vehicles on cancer and mortality in the United States. *Environmental Science & Technology* **2007,** 41, (11), 4150-4157.
11. Organization, W. H., Formaldehyde. **1989**.
12. Bergthorson, J. M.; Thomson, M. J., A review of the combustion and emissions properties of advanced transportation biofuels and their impact on existing and future engines. *Renewable and sustainable energy reviews* **2015,** 42, 1393-1417.
13. Heck, d. H. A.; Casanova, M.; Starr, T. B., Formaldehyde toxicity—new understanding. *Critical reviews in toxicology* **1990,** 20, (6), 397-426.
14. Amitai, Y.; Zlotogorski, Z.; Golan-Katzav, V.; Wexler, A.; Gross, D., Neuropsychological impairment from acute low-level exposure to carbon monoxide. *Archives of neurology* **1998,** 55, (6), 845-848.
15. Ernst, A.; Zibrak, J. D., Carbon monoxide poisoning. *New England journal of medicine* **1998,** 339, (22), 1603-1608.
16. EPA, U. S. Basic Information about NO2. https://www.epa.gov/no2-pollution/basic-information-about-no2#Effects
17. Salvi, S.; Holgate, S., Mechanisms of particulate matter toxicity. *Clinical and experimental allergy* **1999,** 29, (9), 1187-1194.
18. Hosseinpoor, A. R.; Forouzanfar, M. H.; Yunesian, M.; Asghari, F.; Naieni, K. H.; Farhood, D., Air pollution and hospitalization due to angina pectoris in Tehran, Iran: a time-series study. *Environmental Research* **2005,** 99, (1), 126-131.

19. Zettervall, N.; Fureby, C.; Nilsson, E. J. K., Small Skeletal Kinetic Mechanism for Kerosene Combustion. *Energy & Fuels* **2016,** 30, (11), 9801-9813.
20. Lu, T.; Law, C. K., Toward accommodating realistic fuel chemistry in large-scale computations. *Progress in Energy and Combustion Science* **2009,** 35, (2), 192-215.
21. Yalamanchili, S.; Sirignano, W.; Seiser, R.; Seshadri, K., Reduced methanol kinetic mechanisms for combustion applications. *Combustion and flame* **2005,** 142, (3), 258-265.
22. Held, T. J.; Dryer, F. L., A comprehensive mechanism for methanol oxidation. *International Journal of Chemical Kinetics* **1998,** 30, (11), 805-830.
23. Research), M. a. A. E. C., Chemical-Kinetic Mechanisms for Combustion Applications. In University of California at San Diego: http://combustion.ucsd.edu, 2016.
24. Li, J.; Zhao, Z.; Kazakov, A.; Chaos, M.; Dryer, F. L.; Scire, J. J., A comprehensive kinetic mechanism for CO, CH2O, and CH3OH combustion. *International Journal of Chemical Kinetics* **2007,** 39, (3), 109-136.
25. Fomin, A.; Zavlev, T.; Alekseev, V. A.; Rahinov, I.; Cheskis, S.; Konnov, A. A., Experimental and modelling study of 1 CH 2 in premixed very rich methane flames. *Combustion and Flame* **2016,** 171, 198-210.
26. Li, Y.; Zhou, C.-W.; Somers, K. P.; Zhang, K.; Curran, H. J., The oxidation of 2-butene: A high pressure ignition delay, kinetic modeling study and reactivity comparison with isobutene and 1-butene. *Proceedings of the Combustion Institute* **2017,** 36, (1), 403-411.
27. Zhen, X.; Wang, Y., Numerical analysis on original emissions for a spark ignition methanol engine based on detailed chemical kinetics. *Renewable Energy* **2015,** 81, 43-51.
28. Fernández-Tarrazo, E.; Sánchez-Sanz, M.; Sánchez, A. L.; Williams, F. A., A multipurpose reduced chemical-kinetic mechanism for methanol combustion. *Combustion Theory and Modelling* **2016,** 20, (4), 613-631.
29. Seiser, R.; Seshadri, K.; Williams, F. A., Detailed and reduced chemistry for methanol ignition. *Combustion and Flame* **2011,** 158, (9), 1667-1672.
30. Lindstedt, R.; Meyer, M., A dimensionally reduced reaction mechanism for methanol oxidation. *Proceedings of the combustion institute* **2002,** 29, (1), 1395-1402.
31. Liao, S.-Y.; Li, H.-M.; Mi, L.; Shi, X.-H.; Wang, G.; Cheng, Q.; Yuan, C., Development and validation of a reduced chemical kinetic model for methanol oxidation. *Energy & Fuels* **2010,** 25, (1), 60-71.
32. Burke, U.; Metcalfe, W. K.; Burke, S. M.; Heufer, K. A.; Dagaut, P.; Curran, H. J., A detailed chemical kinetic modeling, ignition delay time and jet-stirred reactor study of methanol oxidation. *Combustion and Flame* **2016,** 165, 125-136.
33. Dorigo, M.; Maniezzo, V.; Colorni, A., Ant system: optimization by a colony of cooperating agents. *IEEE Transactions on Systems, Man, and Cybernetics, Part B (Cybernetics)* **1996,** 26, (1), 29-41.
34. Dorigo, M.; Birattari, M.; Stutzle, T., Ant colony optimization. *IEEE computational intelligence magazine* **2006,** 1, (4), 28-39.
35. Turányi, T., MECHMOD: program for the modification of gas kinetic mechanisms. In 2003.
36. *CHEMKIN-PRO 15142*, Reaction Design: San Diego, 2015.
37. Mitchell, M., *An introduction to genetic algorithms*. MIT press: 1998.
38. Balki, M. K.; Sayin, C., The effect of compression ratio on the performance, emissions and combustion of an SI (spark ignition) engine fueled with pure ethanol, methanol and unleaded gasoline. *Energy* **2014,** 71, 194-201.

39. Fieweger, K.; Blumenthal, R.; Adomeit, G., Self-ignition of SI engine model fuels: a shock tube investigation at high pressure. *Combustion and Flame* **1997,** 109, (4), 599-619.
40. Noorani, K. E.; Akih-Kumgeh, B.; Bergthorson, J. M., Comparative high temperature shock tube ignition of C1− C4 primary alcohols. *Energy & fuels* **2010,** 24, (11), 5834-5843.
41. Beeckmann, J.; Röhl, O.; Peters, N. *Experimental and numerical investigation of iso-octane, methanol and ethanol regarding laminar burning velocity at elevated pressure and temperature*; 0148-7191; SAE Technical Paper: 2009.
42. Vancoillie, J.; Verhelst, S.; Demuynck, J. *Laminar burning velocity correlations for methanol-air and ethanol-air mixtures valid at SI engine conditions*; 0148-7191; SAE Technical Paper: 2011.
43. Beeckmann, J.; Cai, L.; Pitsch, H., Experimental investigation of the laminar burning velocities of methanol, ethanol, n-propanol, and n-butanol at high pressure. *Fuel* **2014,** 117, 340-350.
44. Davidson, D. F.; Hanson, R. K., Interpreting shock tube ignition data. *International Journal of Chemical Kinetics* **2004,** 36, (9), 510-523.
45. Naucler, J. D.; Sileghem, L.; Nilsson, E. J.; Verhelst, S.; Konnov, A. A., Performance of methanol kinetic mechanisms at oxy-fuel conditions. *Combustion and Flame* **2015,** 162, (5), 1719-1728.

Supporting Information

ACR55.txt: The reduced mechanism input file developed in this work.

ACR55-therm.txt: The thermodynamic data associated with the reduced mechanism.

ACR55-trans.txt: The transport data associated with the reduced mechanism.

CH3OH_supporting_information.pdf: Additional validation figures, showing cases that was not included in the main text, modified reaction rates, and sensitivity analysis for relevant cases discussed in the main text. Figures show results simulated at conditions from the validation set of Table 1.